

# Comparison of plane grating monochromators

A computer programme for the ray-trace analysis of plane grating monochromators is described. A detailed comparison among various arrangements using  $f/5$  mirrors was made and requirements for slit curvature are considered.

## 1. Introduction

Many publications have appeared before, describing grating monochromators in terms of spot diagrams. Although various types of monochromators have been dealt with extensively it appeared necessary to make a comparison among the different arrangements with similar overall dimensions. A computer programme prepared for plane grating monochromators was used to calculate the corresponding spot diagrams for zero order and finite wavelength.

The following types of monochromators have been investigated:

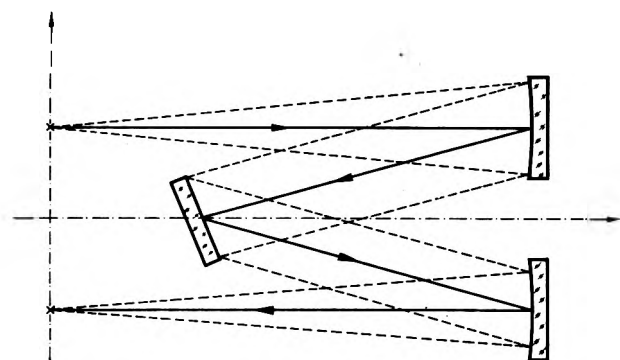


Fig. 1. Czerny-Turner monochromator

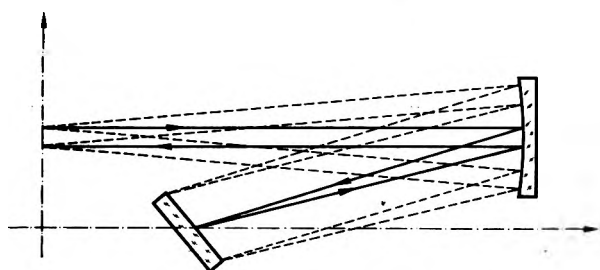


Fig. 2. Littrow monochromator

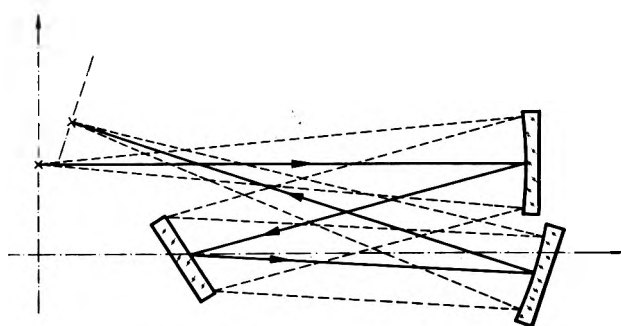


Fig. 3. Chupp-Grantz arrangement

Czerny-Turner monochromator with both spherical and parabolic mirrors (fig. 1); the Littrow system with both spherical and parabolic mirrors (fig. 2); the Chupp-Grantz arrangement [1] (fig. 3).

The common dimensions chosen for all the types are: focal length of 320 mm for both spherical and parabolic mirrors and a grating size of  $60 \times 60$  mm. The specific dimensions (distances of mirrors etc.) were chosen as to minimize the off-axis angles without introducing additional elements. This allows to obtain a general purpose monochromator with a  $f$ -number of about 5. In the calculations for finite wavelength we have assumed a grating with 600 groves/mm used in the first order to cover the UV-visible range. This, however, is not a restriction since it is only the actual grating angle that is important and the results can be easily interpreted for other wavelengths.

## 2. The computer programme

For a given system the grating can be considered as the limiting aperture. The rays, emerging from one point of the slit are chosen so, that they cover the grating uniformly, forming a regular matrix on

\* Hungarian Optical Works, Budapest, Hungary.

the grating. The principal rays passing through the grating centre are found by iteration. In the calculations the slits are taken as infinitely narrow. Since all the types of monochromators considered are symmetrical about a plate, it was sufficient to carry out the calculations for only one-half of the slit length. Separate subprogrammes were made for tracing a ray through parabolic and spherical mirrors and the grating (the latter includes the case of a plane mirror). A focusing subprogramme was prepared, similar to that described by HOROWITZ [2] which automatically finds the best image plane, where the extent of the spot in a direction perpendicular to the exit slit is minimum. For a particular arrangement the programme was assembled by using these subprogrammes.

### 3. Results

Fig. 4 shows the spot diagrams for Czerny–Turner arrangement with spherical mirrors for zero order ( $\lambda = 0$ ) and  $\lambda = 1 \mu\text{m}$ . The distance  $\Delta f$  from the Gaussian focal plane to the best image plane has

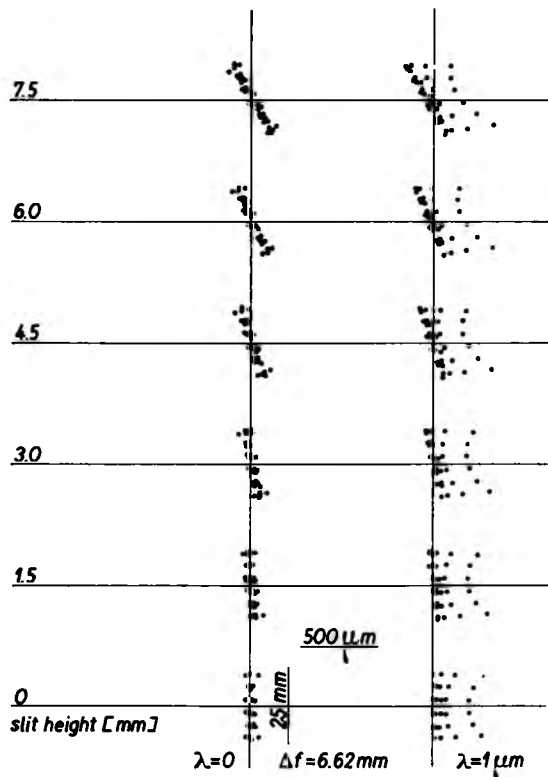


Fig. 4. Spot diagrams for the Czerny–Turner system with spherical mirrors. The vertical scale of the spots are compress by a factor of 5 to avoid overlapping between neighbourin slit points due to the large astigmatism.  $\Delta f$  is the image plane – Gaussian plane distance

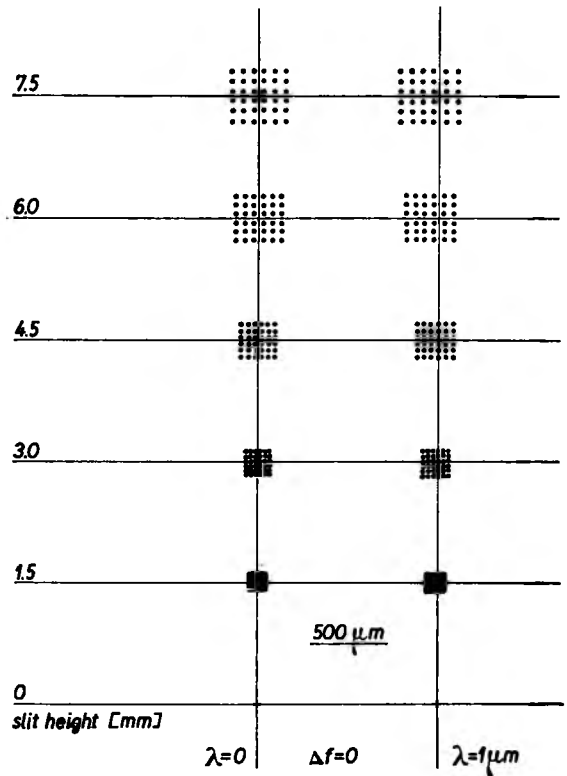


Fig. 5. Spot diagrams for the Czerny–Turner system with parabolic mirrors

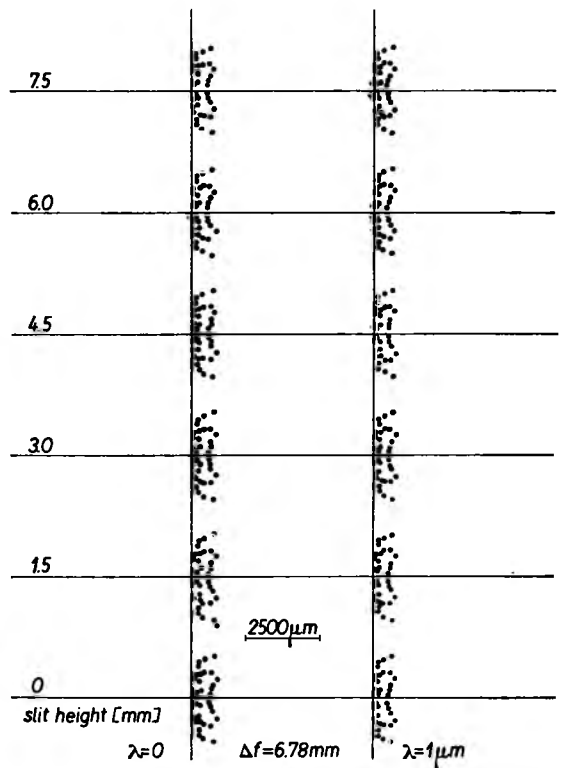


Fig. 6. Spot diagrams for the Littrow system with spherical mirror

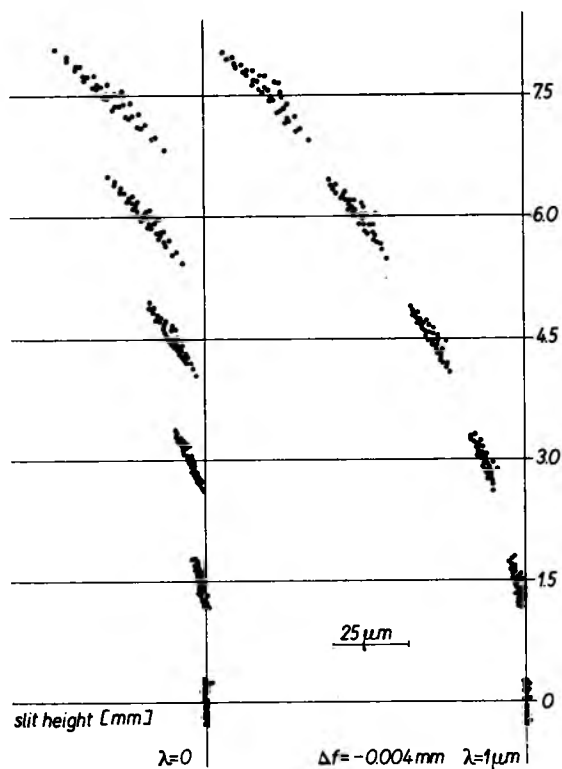


Fig. 7. Spot diagrams for the Littrow system with parabolic mirror

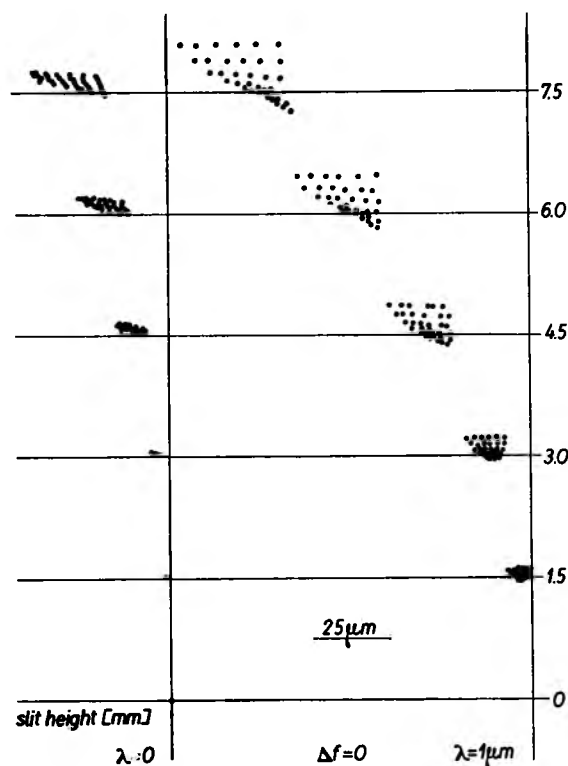


Fig. 8. Spot diagrams for the Chupp-Grantz system

also been indicated in this diagram. Fig. 5 shows the corresponding distribution for the arrangement with parabolic mirrors. It can be seen that, though the imaging is perfect for zero slit height, the image rapidly deteriorates for finite slit height. Figs. 6 i 7 show the Littrow monochromator with spherical and parabolic mirrors. The latter arrangement is now far more superior for all practical slit heights. (Notice the different scales for the two diagrams). In fact, the Littrow parabolic arrangement can be compared in performance only with the Chupp-Grantz monochromator, the spot diagrams for which are shown in fig. 8. This arrangement combines the good imaging capabilities of a Littrow parabolic system with the wavelength independent slit curvature that can be realised in FASTIE monochromator [3]. The spot diagram results for Fastie monochromators are similar to the spherical mirror Czerny-Turner arrangement with which it in fact coincides if the slits are in the plane of the grating.

#### 4. Curvature of slits

In the case of a straight entrance slit the wavelength-dependent curvature of spectral lines is given approximately by the following formula [4]:

$$R = \frac{f}{2} \left[ \sqrt{\left( \frac{2a \cos \Phi}{m\lambda} \right)^2 - 1} - \tan \Phi \right], \quad (1)$$

where  $a$  is the grating constant,  $m$  — the spectrum order,  $\lambda$  — the wavelength,  $f$  — the mirror focal length, and  $\Phi$  — the half of the principal ray separation angle at the grating.

Fig. 9 illustrates the curved spectral lines in a Littrow parabolic monochromator. We obtained the data by means of the ray tracing programme using only the principal rays. This is possible since coma is negligible for this system. The curvature at  $\lambda = 0$  is due to the distortion of optical system which is not contained in equation (1). As we shall see later, it is practically impossible to realise curved slits to obtain wavelength invariance in a Littrow monochromator. The only possible correction is to choose a curved exit (or entrance) slit that fits to the middle of the wavelength range. The results is shown in fig. 10.

The wavelength-invariant slit curvature was examined in the case of the Chupp-Grantz monochromator. By taking into consideration straight slits we obtain images of different curvature, similarly to those of the Littrow system. If both the entrance and

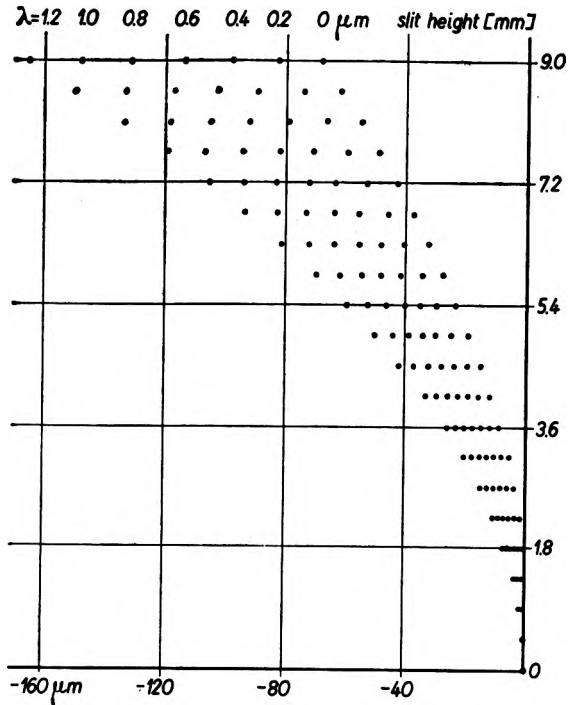


Fig. 9. Curved spectrum lines. Littrow system. Straight slit

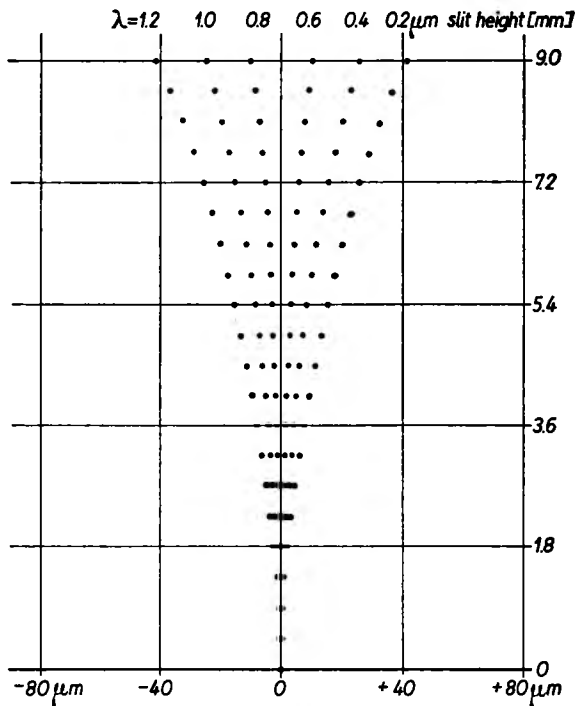


Fig. 10. Curved spectrum lines related to the exit slit. Littrow system. Straight entrance slit, curved exit slit.  $R=328$  mm

exit slits are curved, i.e.

$$R = f \tan \Phi, \quad (2)$$

then the image will be independent of the wavelength (fig. 11). This condition can be derived from the three-

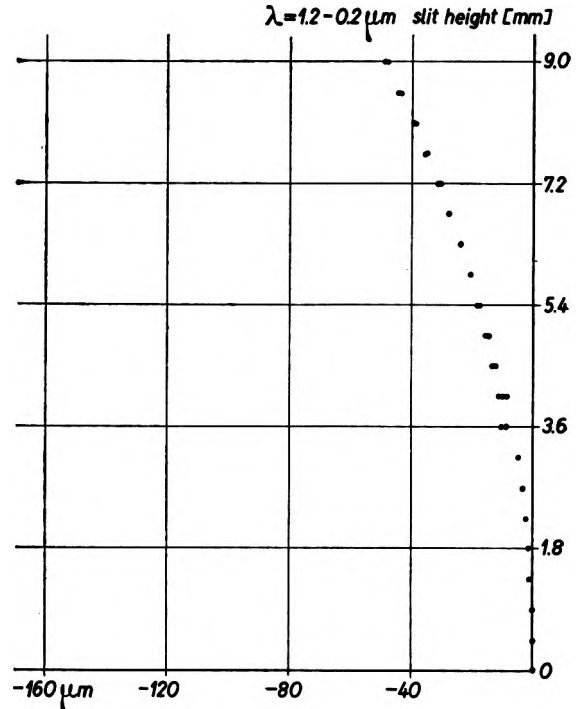


Fig. 11. Spectrum lines with wavelength independent curvature related to the exit slit. Chupp-Grantz system. Curved slits.  $\Phi = 90^\circ$ ,  $R = 48.13$  mm

-dimensional grating equation [5]. A simplified derivation is given in the Appendix. By using off-axis parabolic mirrors in the Chupp-Grantz monochromator, the angle  $\Phi$  may be large enough to permit the usage of appropriately long slits. In the Littrow system the angle  $\Phi$  is too small to allow a practically usable slit height.

If both entrance and exit slits are of equal curvature the wavelength invariance is realizable but in consequence of the distortion of the system the curvature of the exit slit is not exactly the same as that of spectral lines (fig. 11). This problem can be solved by using different curvatures for slits ( $R_{ent} = 48.13$  mm,  $R_{ex} = 52.16$  mm).

### Appendix

Grating equation (symbols are given in fig. 12):

$$\sin \alpha' + \sin \alpha = \frac{m\lambda}{a \cos \gamma},$$

$$\gamma' = -\gamma; \quad (I)$$

for the centre of the slit it takes the form:

$$\sin \alpha'_0 + \sin \alpha_0 = \frac{m\lambda}{a}. \quad (II)$$

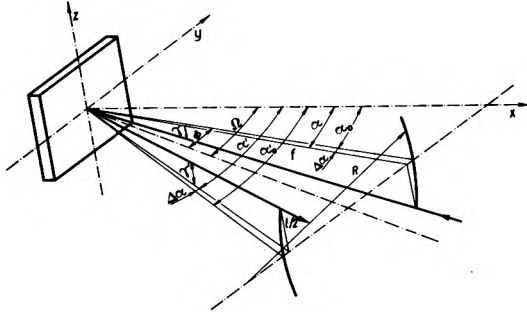


Fig. 12. Ray path for slit curvature

From fig. 12 we have

$$\Delta\alpha = \frac{l^2}{8Rf},$$

$$\alpha' = \alpha_0 - \Delta\alpha,$$

$$\alpha = \alpha_0 + \Delta\alpha.$$

Substituting into (I) we have

$$\sin\alpha_0' + \sin\alpha_0 + \frac{l^2}{8Rf} (\cos\alpha_0 - \cos\alpha_0') = \frac{m\lambda}{a\cos\gamma}.$$

Introducing the angles  $2\Omega = \alpha_0' + \alpha_0$ ,  $2\Phi = \alpha_0' - \alpha_0$  from (II) we have

$$2\sin\Omega\cos\Phi + \frac{l^2}{8Rf} 2\sin\Omega\sin\Phi = \frac{m\lambda}{a\cos\gamma}.$$

### Comparison of... monochromators

$$1 + \frac{l^2}{8Rf} \tan\Phi = \frac{1}{\cos\gamma}.$$

Since  $\gamma \approx \frac{l}{2f}$ , we have finally  $R = f \cdot \tan\Phi$ .

### Сравнение монохроматоров с плоскими сетками

Описана программа ЭЦВМ для анализа пути лучей в монохроматорах с плоской сеткой. Сравнены две схемы, в которых применены зеркала, и приведены требования относительно кривизны щели.

### References

- [1] CHUPP V. L., GRANTZ P. C., Appl. Opt. **8**, 5, 925 (1969).
- [2] HORWITZ J. W., Optica Acta, **21**, 3, 169 (1974).
- [3] FASTIE W. G., J. Opt. Soc. Am. **42**, 9, 647 (1952).
- [4] STROKE G. W., Encyclopedia of Physics (ed. S. Flüge), Springer-Verlag, Berlin, Heidelberg, New York 1967, Vol. 20, p. 467.
- [5] RUPERT C. S., J. Opt. Soc. Am. **42**, 10, 779 (1952).

Received, October 12, 1977